

Summary of the Delft University Wind Turbine Dedicated Airfoils

W. A. Timmer

e-mail: w.a.timmer@citg.tudelft.nl

R. P. J. O. M. van Rooij

e-mail: r.vanrooij@citg.tudelft.nl

Delft University Wind Energy Research Institute,
Faculty of Civil Engineering and Geosciences
Stevinweg 1, 2628 CN Delft, The Netherlands

This paper gives an overview of the design and wind tunnel test results of the wind turbine dedicated airfoils developed by Delft University of Technology (DUT). The DU-airfoils range in maximum relative thickness from 15% to 40% chord. The first designs were made with the XFOIL code. The computer program RFOIL, which is a modified version of XFOIL featuring an improved prediction around the maximum lift coefficient and the capability of predicting the effect of rotation on airfoil characteristics, has been used to design the airfoils since 1995. The measured effect of Gurney flaps, trailing edge wedges, vortex generators (vg) and trip wires on the airfoil characteristics of various DU-airfoils is presented. Furthermore, a relation between the thickness of the airfoil leading edge and the angle-of-attack for leading edge separation is given. [DOI: 10.1115/1.1626129]

Introduction

During the last decade some fifteen wind turbine airfoils have been designed at DUT, of which five have been extensively tested in the Delft University wind tunnel (LST) and four in the low-speed wind tunnel of IAG Stuttgart. Two designs were tested in both wind tunnels to verify specific design features.

The goal of the LST-tests was twofold. First, they served as a validation of the design code and a verification of the capabilities of the code to predict specific airfoil features. Furthermore, the effect on performance of aerodynamic devices such as Gurney flaps and vortex generators could be studied experimentally. As a result, the airfoil designs are well documented and constitute a series of base airfoils from which other designs may be derived with confidence.

The general designation of the DU airfoils is DU yy-W-xxx, in which DU stands for Delft University, followed by the last two digits of the year in which the airfoil was designed. The W denotes the wind energy application, to distinguish the airfoil from the ones designed for sail-planes and general aviation. The last three digits give 10 times the airfoil maximum thickness in percent of the chord. In the case of DU 91, there is an additional number following the W to denote that there has been more than one design with a thickness of about 25% that year.

At present, DU airfoils (Fig. 1), with a relative thickness ranging from 15% to 40%, are being used by various wind turbine manufacturers world wide in over 10 different rotor blades for turbines with rotor diameters from 29 m to over 100 m, corresponding to machines with maximum power ranging from 350 kW to 3.5 MW.

In the 1980s and early 1990s, it was common practice to use existing airfoil families like the four-digit NACA 44 and the six-digit NACA 63 series for the design of wind turbine blades. The required thickness in the root was achieved by linearly scaling the coordinates from airfoils with smaller thickness. From calculations and wind tunnel tests, it appeared, however, that the thick members of the NACA airfoil family suffer from a severe degradation of the performance due to premature transition. In this period, research projects were conducted in various institutes in the United States and Europe (e.g., [1,2]) to produce alternatives for the widely used NACA airfoils, especially those with a maximum relative thickness of 21% or more. Three DU-airfoils result from this period, designated DU 91-W1-251, DU 91-W2-250, and DU 93-W-210.

In practice, most wind turbine manufacturers tune the blades of

stall-regulated machines with vortex generators and stall strips. Furthermore, Gurney flaps apply, possibly in combination with vortex generators. In the Delft wind tunnel, tests were performed (mostly on airfoil DU 93-W-210) to answer the resulting quest for data concerning the effect on airfoil performance and to give guidelines for locations and sizes of the various tuning devices.

With the growing knowledge of the mechanism behind wind turbine blade noise and the effect of rotation (although not yet fully understood) during the second half of the 1990s, a number of airfoils were designed using an 18% thick tip airfoil with low maximum lift (DU 95-W-180) and a 30% thick inboard airfoil (DU 97-W-300) as base lines.

The work on wind turbine airfoils at Delft University has been the subject of a number of contributions to consecutive European wind energy conferences, e.g. [3–6], where some of the subjects discussed in this paper can be found in more detail. In the following, the design philosophy and some experimental results for the DU airfoils will be presented.

Prediction of the 2-D Airfoil Characteristics

Modifications to XFOIL. The XFOIL code (version 5.4) was used to design the earlier Delft airfoils. From 1995, predictions were performed with RFOIL. The RFOIL code resulted from a project called TIDIS (Three-Dimensional Effects in Stall), funded by the Netherlands Agency for Energy and the Environment (NOVEM) and carried out by the Netherlands Energy Research Foundation ECN, the National Aerospace Laboratory NLR and Delft University. The goal of TIDIS was to generate a code to calculate the effect of rotation on airfoil performance using the strong viscous/inviscid interaction scheme of XFOIL. To this end, first the code's prediction of the airfoil performance around the 2-D maximum lift was enhanced. Improvement of the numerical stability was achieved by using the Schlichting velocity profiles for the turbulent boundary layer instead of Swafford's. Furthermore, the shear lag coefficient in Green's lag entrainment equation of the turbulent boundary layer model was adjusted and deviation from the equilibrium flow was coupled to the shape factor of the boundary layer [7].

In Fig. 2, a comparison is made between the "old" XFOIL version 5.4, the latest version 6.94 and RFOIL. Version 5.4 had a convergence problem around $C_{l,max}$, which was solved in one of the later versions. However, it produced a maximum lift coefficient closer to the wind tunnel value than the most recent version. The RFOIL result follows the measured lift curve fairly well. The drag, however, remains under predicted and the lift gradient is too steep. The code tends to over predict the effect of a finite trailing edge on the lift curve. The lift curve is better predicted using half

Contributed by the Solar Energy Division of THE AMERICAN SOCIETY OF MECHANICAL ENGINEERS for publication in the ASME JOURNAL OF SOLAR ENERGY ENGINEERING. Manuscript received by the ASME Solar Energy Division February 27, 2003; final revision July 7, 2003. Associate Editor: D. Berg.

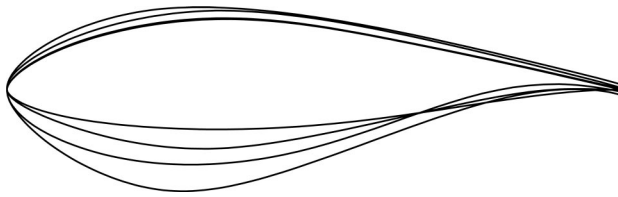


Fig. 1 A series of DU airfoils for a pitch regulated 55 m diameter rotor

the trailing edge thickness. For airfoils with a gradual stall, like DU 91, the $C_{l,max}$ and the trend in post-stall (time-averaged) lift are fairly well predicted.

Rotational Effects. The integral boundary layer equations in XFOIL have been extended for radial flow based on the Snel-Houwink model for blade rotation. [8]. A Johnston cross-flow velocity profile and additional closure relations were added. In order to ensure convergence of the calculation, adjustments were limited to first and second order terms. The cross-terms in the 3-D boundary layer equations are driven by the local solidity c/r , which is used as an input parameter.

The predictive value of RFOIL calculations has been verified against, among others, measurements performed by FFA on a 5.35 m diameter model rotor in the 12×16 m. low-speed wind tunnel of the Chinese Aerodynamics Research and Development Center, CARDC. The rotor blades incorporated the NACA 44 series of airfoils. Pressure distributions at various span locations were measured and integrated to yield normal force and tangential force coefficients C_n and C_t . Because the angle-of-attack during the experiments was not known, a match has been made between the measured C_n-C_t curves and those calculated by RFOIL. It was established that RFOIL tends to overestimate the rotational effect for a specific c/r value. Nevertheless, if 2/3 of the geometrical c/r value was used, it appeared that RFOIL was capable of predicting the pressure distribution on the rotating blade quite well. In Fig. 3, an example is given of the measured and calculated pressure distributions for a matched point in the C_n-C_t curve of the 30% span section at a Reynolds number of 420,000. The predicted C_n and C_t values originate from a calculation of airfoil NACA 4424 at an angle-of-attack of 18 deg. The same trend emerged from comparisons with pressure distributions measured on the blades of the 10 m. diameter two-bladed rotor of the Delft University field test installation. The blades incorporate the NLF (1)-0416 airfoil.

It was felt that RFOIL could be used to generate airfoils for the inner 40% of the blade span and predict trends in roughness sensitivity and height of $C_{l,max}$ with airfoil thickness to a reasonable degree.

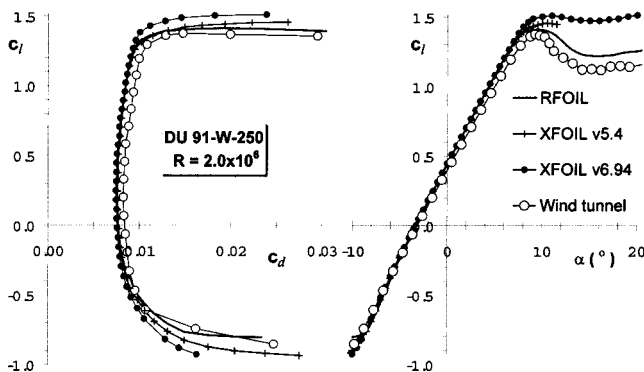


Fig. 2 The predicted DU 91-W2-250 characteristics with two versions of XFOIL and with RFOIL

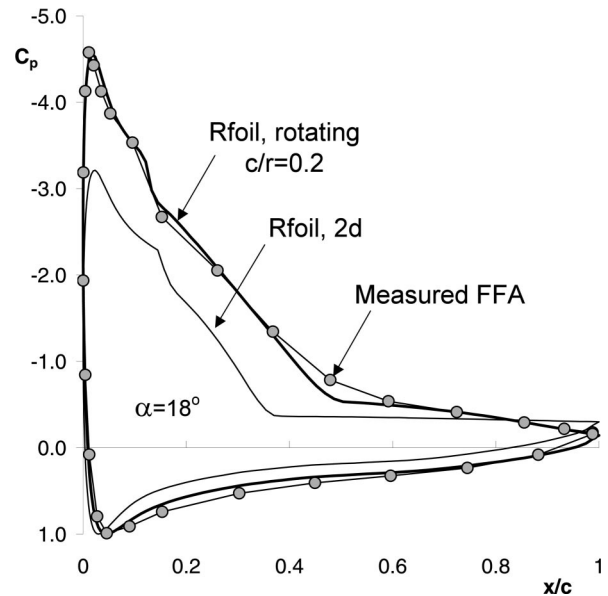


Fig. 3 The predicted and measured effect of rotation on the pressure distribution of the 30% span section of a rotating blade

Experimental Setup and Procedure

Wind Tunnel. The tests reported here were performed in the low-speed, low-turbulence wind tunnel of the Faculty of Aerospace Engineering of Delft University, Fig. 4. The wind tunnel is of the closed single-return type with a total circuit length of 72.7 m. The circuit has a contraction ratio of 17.8 to 1. The free-stream turbulence level in the 2.6 m long, 1.25 m high, and 1.80 m wide octagonal test section ranges from 0.02% at a wind speed of 25 m/s to 0.07% at 75 m/s. These wind speeds correspond to Reynolds numbers in the range from 1×10^6 to 3×10^6 , using 0.6 m chord models.

A 580 kW DC motor, giving a maximum test section velocity of about 120 m/s, drives a 2.9 m diameter six-bladed fan. Electrically actuated turntables flush with the test-section top and bottom wall provide positioning and attachment for a 2-D model.

Models. The composite models had a chord of 0.6 m and completely spanned the height of the test section. Around 90 to 100 pressure orifices with a diameter of 0.4 mm. were installed in staggered formation. The polyester gelcoat surface of the models was sanded and polished. The model contour of the airfoils presented here was not measured. However, the deviation from the

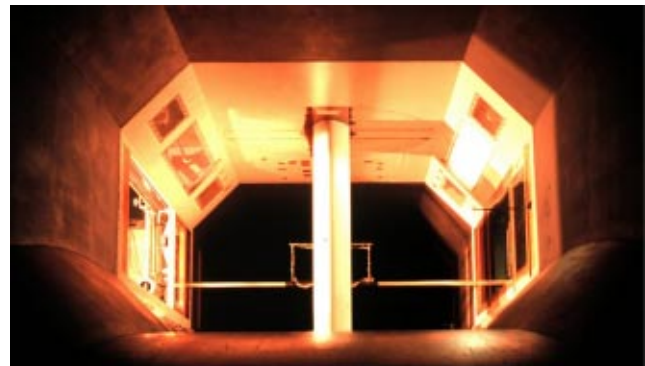


Fig. 4 The model of airfoil DU 97-W-300 in the LST test section seen from inside the contraction. The wake rake is in the back.

prescribed shape of similar wind tunnel models from the same manufacturer has always been well below 0.1 mm.

Instrumentation. The model static pressures and the wake rake static and total pressures were fed either to an electronically read 200 tube liquid multi-manometer with fiber optic cells or an electronic pressure scanner system. Data were recorded using an electronic data acquisition system and were on line processed using the laboratory computer.

During the years, a variety of wake rakes has been used ranging from a device with 50 total tubes and 12 static tubes with a width of 219 mm. to the present one having 67 total pressure tubes and 16 static pressure tubes over a length of 504 mm.

Force Coefficients. The testing of each new model configuration started with a number of wake rake traverse measurements in span wise direction at various angles-of-attack and Reynolds numbers to confirm the two-dimensionality and to establish the wake rake position, giving an average drag value representative for the model. The model pressure distributions were integrated to obtain normal force and tangential force coefficients C_n and C_t and moment coefficients C_m . Lift coefficients were computed using C_n and the wake rake drag according to Eq. 1. In the post stall region the pressure drag was used, computed from the pressure distributions.

$$C_l = C_n / \cos \alpha - C_d * \tan \alpha \quad (1)$$

Wind Tunnel Wall Corrections. The measured data were corrected for the presence of the wind tunnel walls with the standard correction method for lift-interference and model solid and wake blockage [9]. Corrections have also been made for the effect of solid blockage of the wake rake on the test section velocity and the effect of the wake rake self-blockage on the values of the static pressures (and consequently the dynamic pressure) measured by the wake rake.

The standard position of the wake rake was about 60% chord length downstream from the model trailing edge.

Effects of Roughness. As a standard way to check the sensitivity of the designs to contamination of the leading edge, 0.35 mm thick zigzag tape was used. The tape leading edge was located at the model upper surface 5% chord station.

To trip the boundary layer at this chord position, a grit roughness height of about 0.16 mm would be sufficient, as calculated by the method of Braslow [10]. This value applies to all airfoils tested, at angles around the design angle of attack, using a Reynolds number based on grit roughness height of 600. Zigzag tape is more effective in triggering transition and critical Reynolds numbers based on tape thickness of about 200 have been reported. Using the latter Reynolds number value, a critical zigzag tape thickness of 0.09 mm is calculated.

The zigzag tape of 0.35 mm thickness is not only an effective trip but due to its oversize significantly increases the boundary layer and the momentum thickness. As a result the airfoil is decambered considerably. The effect of the heavy upper surface trip on the characteristics is regarded as a fair indication of the ability of the airfoil to withstand a thick turbulent boundary layer along the suction side starting on the nose. For thick wind turbine airfoils, however, this approach may seriously underestimate the loss in lift due to a rough leading edge. Compared to the suction side, the increased lower surface thickness and the aft loading make the pressure side equally sensitive to tripping. In this case, an additional (severe) trip on the lower surface nose is necessary.

General Design Considerations

Although the design characteristics of a wind turbine airfoil are a trade-off between several conflicting requirements, some properties (such as a high lift-drag ratio) can be identified as being generally desirable. The objective to keep the sensitivity of the airfoil to contamination and contour imperfections of the nose as

low as possible has been the primary design driver for the Delft airfoils. To accomplish this, transition must be on the airfoil nose when approaching stall. A complicating factor for the DU-airfoil designs presented here was the requirement, that the airfoils should fit both fixed and variable blade pitch machines, which meant some compromising regarding the different demands for stall and post stall behavior.

Outboard Airfoils. From the performance perspective, the height of the C_l for maximum lift-drag ratio (the design- C_l) for the outboard airfoils of a pitch controlled wind turbine is relatively unimportant. The difference between the design- C_l and the $C_{l,max}$ must not be too large to prevent excessive loads in case of gusts and not too small to prevent the rotor from stalling when the controller is not fast enough. A difference between the design- C_l and the $C_{l,max}$ of about 0.2 is expected to be sufficient. In the case of a turbine using stall-control, a high $C_{l,max}$ is advantageous since this leads to smaller chords and to lower storm loads. However, airfoils with a high $C_{l,max}$ tend to have a more abrupt stall and larger losses in post stall lift, increasing blade dynamic excitations. Furthermore, for an airfoil with a high $C_{l,max}$ the associated angle-of-attack in case of roughness will be reduced by several degrees, giving large differences in lift at post stall angles between the contaminated and the clean airfoil. The loss in rated power due to roughness of a fixed pitch turbine is proportional to these differences in lift. To avoid this, and to ensure gentle stall characteristics and minimize negative aerodynamic damping, the maximum lift capacity of the designs has been held at a moderate level. Although the design Reynolds number is in the range of 2×10^6 to 4×10^6 , this opens the possibility to use the airfoils in larger blades and consequently at higher Reynolds numbers as well.

Inboard Airfoils. For structural reasons, significant section thickness is required in the root of the blade. Small root chords and restricted blade weight help to overcome problems of transportation of large blades and keep down structural loads on the shaft and bearings. This calls for airfoils with a high relative thickness, typically 30% to 40% chord. The inboard segment of the blade requires a high maximum lift coefficient to deliver sufficient torque at the lower wind speeds. To achieve high lift, the inner 50% span of the blades of stall controlled wind turbines is generally fitted with vortex generators (vg) and numerous wind tunnel tests have revealed that vg can easily boost the maximum lift coefficient to over 1.9.

Thick airfoils are in that part of the blade subjected to rotational effects. To take the design process of thick airfoils one step further than the 2-D approach, a tool to quantify the effects of rotation on the clean and contaminated airfoil is required. As mentioned before, RFOIL is believed to be such a tool.

A summary of measured key parameters of the DU airfoils is listed in Table 1. In the following, the airfoils will be discussed in chronological order.

DU 91-W2-250. The design of airfoil DU 91-W2-250 followed wind tunnel tests on a 25% thick NACA airfoil from the 63-4xx series linearly scaled from 21% [11], designated 63₍₄₂₁₎-425. These tests showed a reduction in the maximum lift coefficient of 35% due to a tripped boundary layer on the 5% upper-surface chord station. The poor performance of thick NACA-airfoils with leading edge contamination can be traced to the high upper-surface velocities and resulting high adverse pressure gradients due to the larger upper-surface thickness, giving premature transition and early separation. The thick airfoils currently in use by most blade manufacturers all have a restrained upper surface thickness to avoid this premature turbulent separation. To compensate for the resulting reduced lift of the upper surface, a certain amount of lower-surface aft loading is incorporated, giving the typical S-shape of the pressure side. It was the intention to use the new 25% thick DU-airfoil in stall as well as

Table 1 Measured key features for various DU-airfoils at a Reynolds number of 3×10^6 . Zigzag tape thickness is 0.35 mm

Airfoil	t/c	Airfoil clean				Zigzag tape at x/c=0.05 u.s.	
		α_0	$C_{l,\alpha}$	$C_{l,max}$	$(C_l/C_d)_{max}$	$C_{l,max}$	$(C_l/C_d)_{max}$
DU 91-W2-250	0.25	-3.2	0.126	1.37	128	1.16	62
DU 93-W-210	0.21	-4.2	0.123	1.35	143	1.17	65
DU 95-W-180	0.18	-2.0	0.116	1.21	143	1.14	70
DU 96-W-180	0.18	-2.7	0.115	1.26	145	1.17	73
DU 97-W-300	0.30	-2.2	0.128	1.56	98	1.17	53

pitch blades for 500 kW machines with rotors of about 40 m diameter, which was still fairly large in the early 1990s. This was translated into the following design goals:

- a design Reynolds number of 3×10^6
- a $C_{l,max}$ of about 1.4 to 1.5 with a gradual stall,
- a $(C_l/C_d)_{max}$ higher than a NACA airfoil with corresponding thickness, $(C_l/C_d)_{max} > 119$
- trailing edge thickness between 0.5% and 1% c for structural reasons
- location of maximum thickness around 30% c

There was no restriction on the moment about the quarter-chord point. The airfoil was designed with the earlier XFOIL version 5.4. Measured pressure distributions are given in Fig. 5 and the measured performance at $R=3 \times 10^6$ is shown in Fig. 6. It ap-

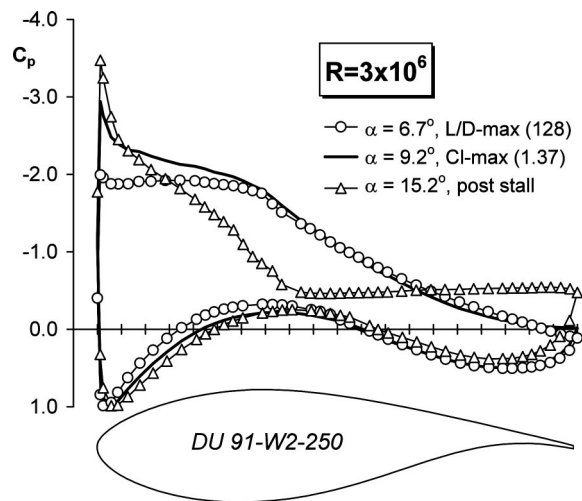


Fig. 5 Measured pressure distributions for DU 91-W2-25 at $R=3 \times 10^6$. Transition free.

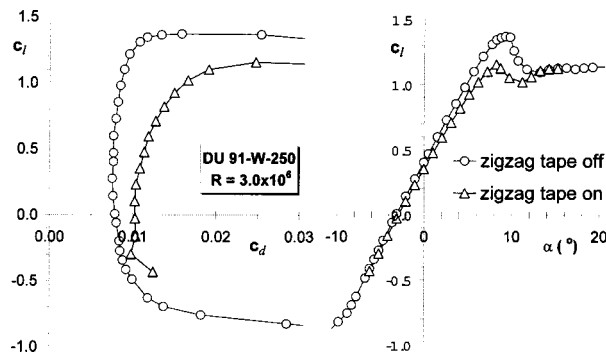


Fig. 6 Measured airfoil performance of DU 91-W2-250 at $R=3 \times 10^6$

peared that the $C_{l,max}$ was just off the target of 1.4, although the calculations predicted a value of 1.53.

The sensitivity of the airfoil to distortion of the boundary layer at the nose was investigated by applying zigzag tape of 0.35 mm thickness at the 5% chord station. Due to the trip the maximum lift coefficient dropped from 1.37 to 1.16. This decrease is less than half the corresponding reduction for the NACA 63₍₄₂₁₎-425 airfoil.

DU 93-W-210. To serve as an intermediate airfoil between DU 91-W2-250 and outboard airfoils with high camber such as NACA 63₃-618, the 21% thick DU 93-W-210 was designed. It should apply to pitch as well as stall regulated machines. The airfoil exhibits a maximum lift-to-drag ratio of 143 at $R=3 \times 10^6$ and a maximum lift coefficient of 1.35. The airfoil model was extensively used to experimentally verify the effect of vg, Gurney flaps and trip wires. Further on in this paper, the results of this investigation will be highlighted. Figure 7 depicts the difference between the contours of DU 91 and DU 93. The upper-surface thickness of the DU 91 airfoil was generally maintained and the airfoil was made more laminar by shifting the location of maximum thickness a few percent backwards in favor of a high lift-to-drag ratio.

In Fig. 8, the maximum l/d and the maximum lift coefficient of DU 93 are depicted. Although the value of $C_{l,max}$ at a Reynolds number of 3×10^6 was a little disappointing (1.35 instead of the predicted 1.45), the overall performance of the airfoil was satisfying. The lift-drag ratio of 143 compares favorably to existing 21% thick airfoils measured at a Reynolds number of 3×10^6 such as NACA 63-421 ($(l/d)_{max}=128$) and S809 ($(l/d)_{max}=113$). Due

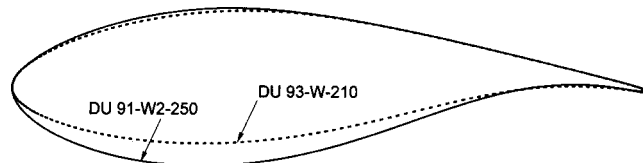


Fig. 7 The airfoil shapes of DU 91-W2-250 and DU 93-W-210

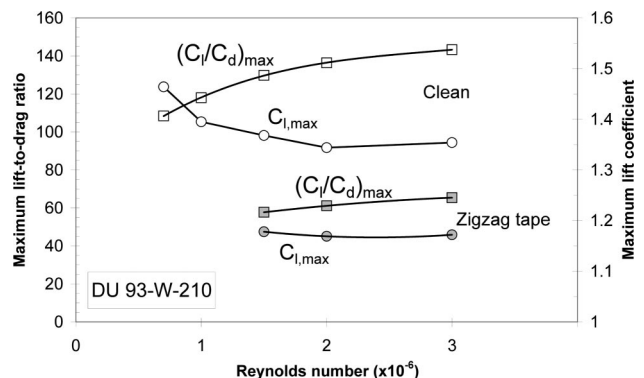


Fig. 8 The effect of Reynolds number on the maximum lift-drag ratio and maximum lift coefficient of airfoil DU 93-W-210

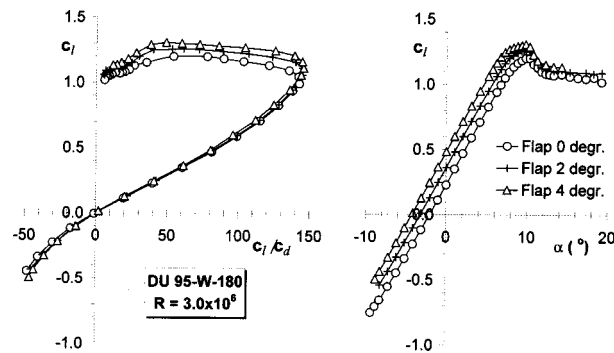


Fig. 9 The effect of a flap deflection on the performance of DU 95-W-180 at $R=3 \times 10^6$

to its high camber, the DU 93 does not match a combination of outboard airfoils like DU 95 or DU 96 and the mid-span DU 91 very well. Alternatively, DU 00-W-212 can be used. This airfoil, however, has not been wind tunnel tested.

DU 95-W-180. For this outboard airfoil, the following requirements were formulated.

- A relative thickness of 18%
- A $C_{l,max}$ of 1.25 at $R=3 \times 10^6$
- A maximum lift-drag ratio of at least 140 at 3×10^6 to compete with existing NACA-airfoils
- A thin trailing edge to avoid excessive boundary layer noise

Wind Tunnel Results. Based on the fact that in earlier designs the $C_{l,max}$ was overpredicted, the wind tunnel model was equipped with a 20% chord trailing edge flap to tune the lift performance.

The measured lift coefficients and accompanying lift-drag ratios of the model with flap deflections of 0 deg, 2 deg and 4 deg for a Reynolds number of 3×10^6 are shown in Fig. 9. The base airfoil (zero flap deflection) appeared to have a maximum lift coefficient of 1.20, instead of the predicted value of 1.25, which however could be reached with a 2 deg flap deflection. The latter configuration was later designated DU 96-W-180 and was also tested at large angles-of-attack in a different test setup [6] and in the low-speed wind tunnel of the Institut für Aero- und Gasdynamik of Stuttgart University (IAG), in Stuttgart Germany. In Fig. 10, measured pressure distributions of DU 96-W-180 from the

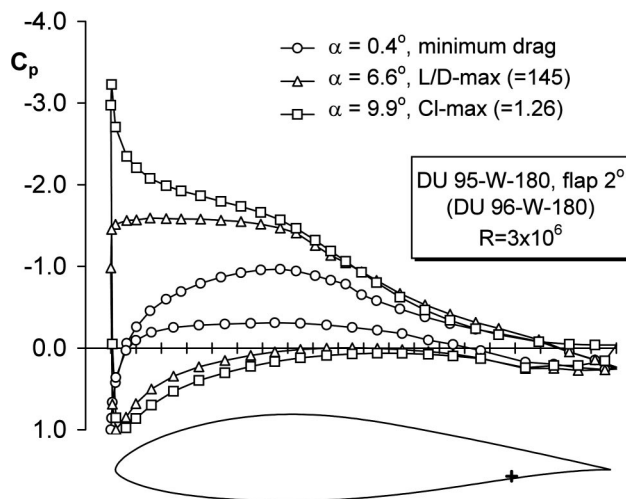


Fig. 10 Measured pressure distributions of airfoil DU 96-W-180 at $R=3 \times 10^6$. Transition free.

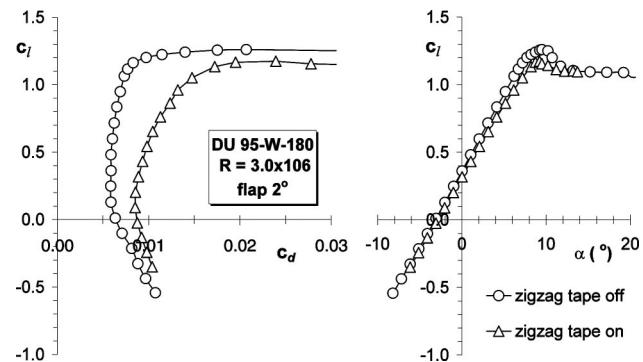


Fig. 11 The effect of zigzag tape at $x/c=0.05$ on the performance of DU 96-W-180

present test are given at angles specific to the airfoil performance. For clarity of the graph, half of the pressure information has been omitted. The airfoil exhibits a high lift-to-drag ratio of 145 at $R=3 \times 10^6$. Measurements in the Stuttgart low-speed wind tunnel at $R=4 \times 10^6$ gave a $(C_l/C_d)_{max}$ of 149 and a $C_{l,max}$ of 1.32. The sensitivity of the airfoil to leading edge roughness is low, as can be deduced from Fig. 11 in which the effect of zigzag tape is shown. The loss in $C_{l,max}$ due to the increased momentum thickness is 0.09.

DU 97-W-300. As a base airfoil for the development of thick airfoils the DU 97-W-300 was designed. Design goals were:

- A $C_{l,max}$ of 1.5 to 1.6 at $R=3 \times 10^6$
- Location of maximum thickness around 30% c
- A thick trailing edge of about 1.5% c for structural reasons
- Span wise position 40% (geometrical c/r about 0.18 to 0.20)
- Smooth transition to DU 91-W2-250
- Acceptable 2-D roughness performance (25% loss in $C_{l,max}$ accepted)

Measured Performance. In Fig. 12, some pressure distributions are shown for specific angles of incidence. The measured

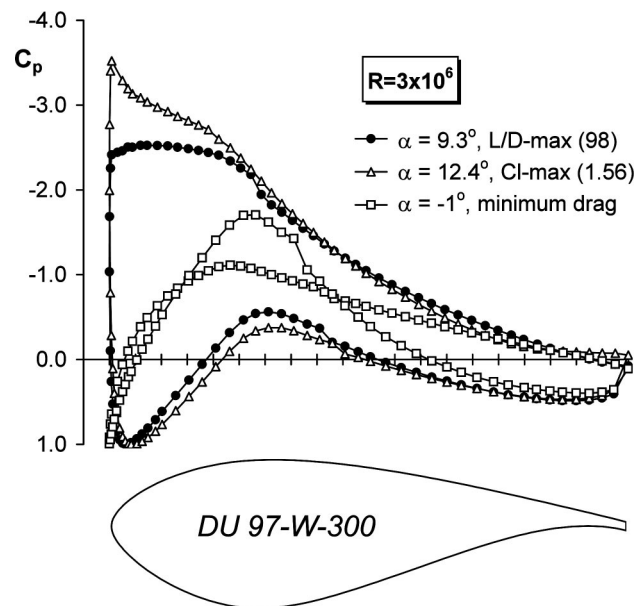


Fig. 12 Measured pressure distributions for airfoil DU 97-W-300 at $R=3 \times 10^6$. Transition free.

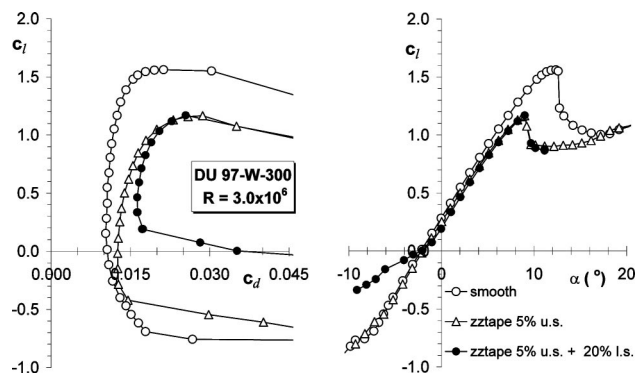


Fig. 13 The effect of zigzag tape on the characteristics of DU 97-W-300 at $R = 3 \times 10^6$

performance of the airfoil both in the transition free and fixed conditions is shown in Fig. 13, for a Reynolds number of 3×10^6 .

Figure 13 demonstrates the effect of zigzag tape on the airfoil performance. The 0.35 mm thick zigzag tape at the 5% chord position reduces the $C_{l,max}$ from 1.56 to 1.16, which is considerable, but nonetheless acceptable for such a thick section. The sensitivity of the lower surface to roughness was investigated by locating 0.25 mm thick zigzag tape on the lower-surface 20% chord position as well. At negative angles, the tape causes separation in an early stage, as indicated by the rapidly increasing drag and decreasing negative lift coefficient.

Predicted Performance. Figure 14 presents the RFOIL prediction for the smooth configuration and for the situation with zigzag tape on both surfaces. In the smooth case, the maximum lift coefficient is well predicted. In the rough condition, the $C_{l,max}$ is over predicted. In the calculation, transition was fixed at 1%c upper surface and 5%c lower surface. It may well be possible that the earlier trip in the calculation (1%c) does not compensate for the increase in boundary layer thickness and momentum thickness introduced by the 0.35 mm thick tape (at 5%c), in which case the boundary layer on the wind tunnel model is much thicker and will separate at a lower angle. In both cases, the measured post stall lift curve drops more abruptly than is predicted. This may be caused by the 3-D flow pattern on the model just after stall. The time averaged pressure distribution only gives local—and in this case too pessimistic—information about this pattern. The predicted separation on the lower surface also starts at angles below 0 deg but the associated effect on lift is more pronounced.

This behavior at negative angles is an indication that the thickness of the lower surface is pushed to the edge of what still is

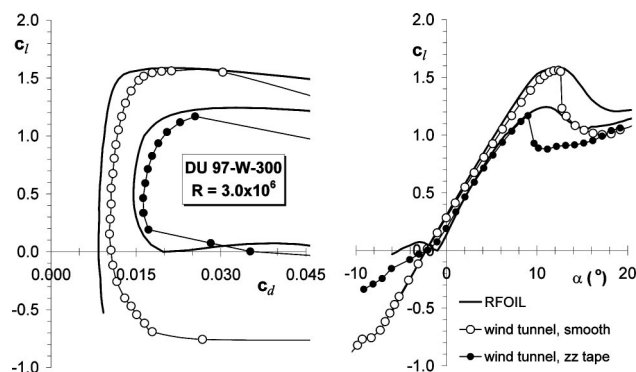


Fig. 14 The measured and calculated performance of DU 97-W-300 at $R = 3 \times 10^6$

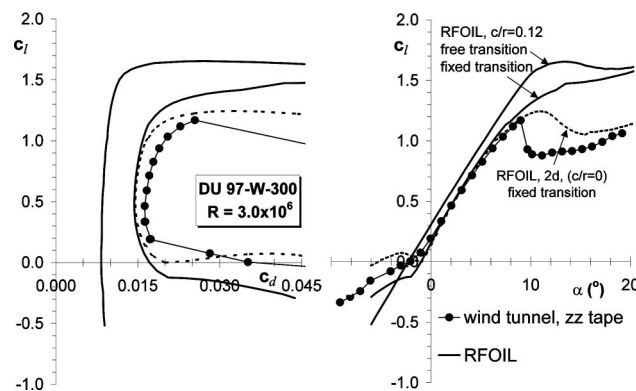


Fig. 15 The RFOIL predicted effect of rotation on DU 97-W-300 in the transition free and fixed condition

acceptable in terms of 2-D airfoil performance. The problem of lower-surface separation could be slightly alleviated by shifting the maximum thickness more forward. This, however, is unfavorable for the location of the spar as well as for transition to the hub. Fortunately, thick airfoils generally do their work at the higher angles-of-attack and rotation helps the boundary layer to overcome a certain pressure rise.

Effect of Rotation. Figure 15 presents the effect of rotation on the characteristics as calculated by RFOIL. The geometric local solidity c/r is in the order of 0.19, assuming that the airfoil is positioned at 40% radius. The figure shows that at this radial position the lift keeps rising continuously in case of a tripped boundary layer. Calculations are performed for 2/3 of the geometrical c/r value. The lift characteristic at the negative angles is enhanced as well, although lower surface separation still comes in quite soon.

Based on the wind tunnel test on DU 97-W-300 and the RFOIL calculations for the 2-D as well as the 3-D configuration, a number of thicker airfoils have been designed for various inboard positions, taking rotational effects into account. Some blade manufacturers have different construction requirements with respect to trailing edge thickness and location of the maximum airfoil thickness, resulting in different sets of inboard airfoils. Recently, DU 00-W-350 and DU 00-W-401 have been tested in the low-speed wind tunnel of the IAG [10]. The 2-D characteristics, both clean and rough, could be relatively well predicted by RFOIL.

The Effect of Aerodynamic Devices

During the wind tunnel measurements the effect of various aerodynamic devices such as Gurney flaps, wedges, trip wires, and vg has been evaluated.

Gurney Flaps. Airfoil DU 93-W-210 was used to investigate the effect of Gurney flaps of 1%c (6 mm) and 2%c (12 mm), the effect of isosceles wedges of 1%, 1.5%, and 2% height and of upstream length of the 1%c high wedges.

Figure 16 presents the effect of Gurney flaps of 1%c and 2%c on the characteristics of DU 93. The Gurney flap was an L-shaped metal strip with a thickness of 2 mm attached to the lower surface trailing edge (see Fig. 17). With the 1%c and 2%c Gurney flap, the maximum lift coefficient was increased by 0.24 and 0.40, respectively. The maximum lift to drag ratio, however, decreased from 136 to 117 and 89, respectively. Figure 16 is a typical example of the effect of 1%c and 2%c Gurney flaps, since the same trend was measured for DU 91-W2-250. It was concluded, and later confirmed by others [12], that for these Reynolds numbers and airfoil shapes, no increase of l/d max would result for Gurney flaps of 1% or higher. In fact, looking at the upper boundary of the low-drag buckets of the three curves on the left hand side of Fig.

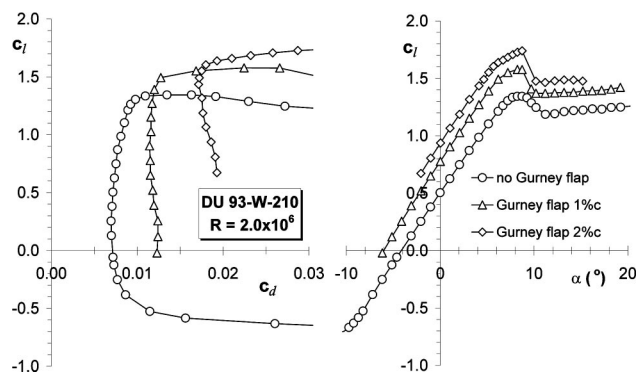


Fig. 16 The effect of 1%c and 2%c Gurney flaps on the performance of DU 93-W-210

16, it is even unlikely that in the clean configuration the l/d will be enhanced by a Gurney flap smaller than 1%. No tests were performed with fixed transition. Given the fact that in those cases the drag is already significantly higher, an increase in l/d might be realized with a small Gurney flap.

Trailing Edge Wedges. To gain more insight in the influence on drag of the separation bubble right in front of the Gurney flap, measurements were performed with 6×6 mm, 6×13 mm, and 6×24 mm. wooden wedges, forming increasingly longer upstream fairings of the basic Gurney flap, see Fig. 17. The test results showed that there was virtually no difference between the characteristics for the 6×6 mm. wedge and the 6 mm high Gurney flap. Apparently the 6×6 mm wedge filled the space otherwise taken by the separation bubble in front of the Gurney flap. Further results are depicted in Fig. 18. It followed that with increasing upstream wedge length the maximum lift coefficient decreased while the maximum lift-to-drag ratio increased. The wedges with a

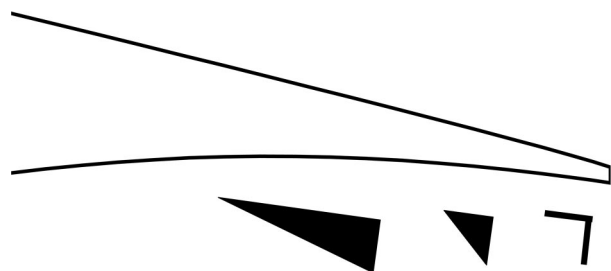


Fig. 17 Sketch of the Gurney flap and some wedges applied to the trailing edge of DU 93-W-210

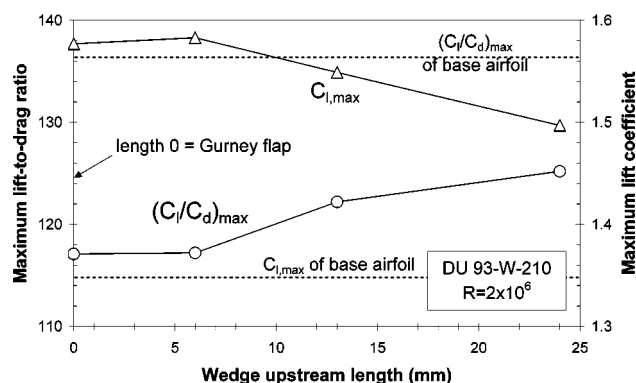


Fig. 18 The effect of wedge upstream length on the $(l/d)_{\max}$ and $C_{l,\max}$ of DU 93-W-210

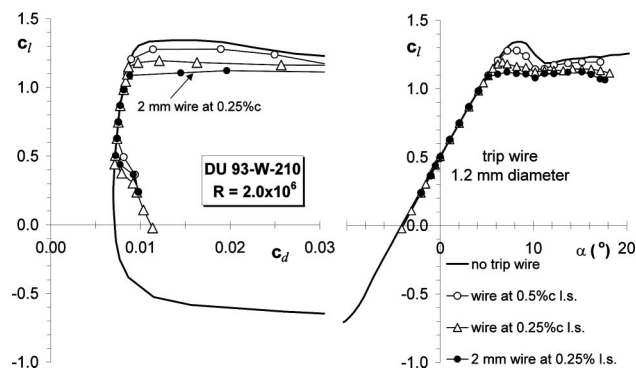


Fig. 19 The effect on performance of thickness and location of a trip wire located on the leading edge of DU 93-W-210

longer upstream length have a smaller effect on the airfoil camber, but at the same time redirect the flow with less base drag.

A general conclusion from the tests with Gurney flaps on DU 93 and DU91 and from the wedge test on DU 93 is that Gurney flaps can be used to significantly increase $C_{l,\max}$ at the cost of a fairly large drag increase. To minimize the negative effect on the maximum lift-to-drag ratio the flap height must be well under 1% chord. The result can be fine tuned by taking a wedge of the same height as the Gurney flap with increased upstream length. Gurney flaps and wedges increase the trailing edge thickness considerably. To avoid undesirable effects on noise, the application of these devices should be restricted to inboard locations.

Stall Strips. Some wind turbine manufacturers tune the blades of stall machines producing too much peak power with stall strips, small metal strips glued to the blade nose to top off the lift performance of the outboard portion of the blade. In many cases, a strip with limited length is enough to trigger the entire blade segment between the strip location and the tip. There was, however, some uncertainty about the proper location and the effect of thickness of the strip. DU 93 was used to perform a wind tunnel test with trip wires on the nose of the model. Wires with 1.2 and 2-mm diameter, respectively, were located at the apex (0%c) and at 0.25%c, 0.5%, and 1% on the pressure side. Some results are presented in Fig. 19.

The measurements show that the 2 mm thick wire at 0.25%c efficiently tops off the maximum lift capacity of the airfoil, since the maximum lift coefficient drops from 1.34 to 1.12. The drag bucket is narrowed significantly. The thinner wire at the same location is not so effective and results in a wider bucket. If the 1.2 mm wire is located at 0.5%c the bucket width remains the same as at 0.25%c but it shifts upward to higher lift coefficients along the drag curve of the base line airfoil. The effect on maximum lift has become smaller. In general terms, the effect of a trip wire can be summarized as follows:

- No effect as long as the wire is in or very near the stagnation point
- The thicker the wire, the narrower the drag-bucket
- The more aft located, the smaller the effect on the maximum lift coefficient
- The range in chord positions for effective application of the trip wire is very small

Vortex Generators (vg). Blades for stall-controlled machines with moderate twist are generally equipped with vortex generators (vg). For the prediction of power curves, the effect of vg was studied on all airfoils tested except DU 95 and DU 96, since these airfoils were meant to be in the outboard section of the blade. The type of vg has always been the same and resulted from a literature study and wind tunnel test in the late eighties. The type is sketched in Fig. 20 and is optimized for the 20%c and 30%c chord

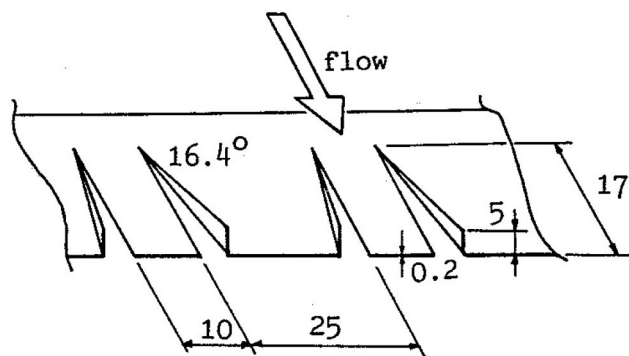


Fig. 20 Sketch of the vortex generators used during most wind tunnel tests. Dimensions in mm.

positions of 0.6 m chord models. It closely resembles one of the types investigated by Wentz [13]. Vortex generators are known to energize the boundary layer, helping it to overcome adverse pressure gradients. The result is suppression of trailing edge separation and consequently the delay of the stalling process of the airfoil. The type shown in Fig. 20 proved to be very effective, and has been successfully applied in practice. In Fig. 21 an example of the test results is shown on airfoil DU 97-W-300. The drag measured with the wake rake showed a regular wavy pattern in span wise direction corresponding to the vane positions. The presented drag is an average value.

The vg placed at 20%*c* increased the maximum lift coefficient of the base airfoil from 1.55 to 1.97, but also increased the drag considerably. Due to the limited radial position of inboard airfoils this will have little effect on the rotor torque. It is worth noting that the effect of premature transition, triggered by zigzag tape at 5%*c*, had little effect on the maximum lift. Apparently, the boundary layer thickness did not grow fast enough to make the vg work less efficient. Rotation has an effect similar to that of vg on the boundary layer of the very inboard stations. This is another indication that, in the design of thick inboard airfoils, roughness (in)sensitivity requirements can be alleviated considerably.

Leading Edge Separation on Wind Turbine Airfoils

At positions around 70% to 80% radius, the flow over the blade behaves more or less 2-D. Dynamic effects may cause leading edge separation, which is linked to multiple-stall levels of a rotor by some researchers. In this light, it was investigated if—with the available test data—the angle-of-attack at which leading edge separation would occur in the static situation could be predicted.

Figure 22 presents the measured lift curves of DU 96-W-180 and DU 97-W-300 at a Reynolds number of 1×10^6 . The sudden

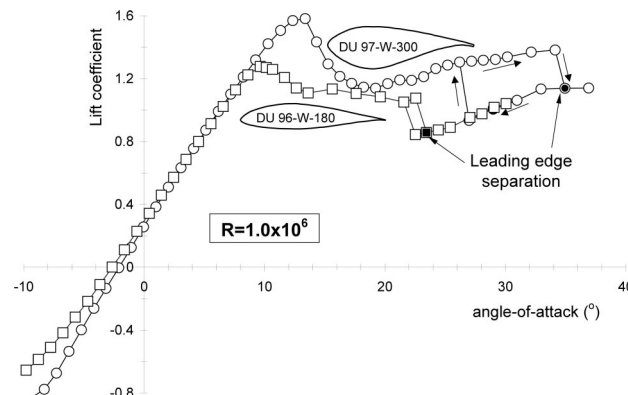


Fig. 22 The lift curves of two DU airfoils showing leading edge separation

drop in lift at 23.4 deg (DU 96-W-180) and 35 deg (DU 97-W-300) is associated with the collapse of the negative pressure peak at the leading edge of the airfoil as a result of the separation process. The angle for leading edge separation (deep-stall) and the length of the hysteresis loop of the two airfoils differ considerably. In Fig. 23, the available data have been correlated with the thickness of the airfoil nose, defined as the *y/c* value at *x/c*=0.0125, following the same procedure as Gault [14], who correlated the stalling characteristics with geometry of a large number of low-speed airfoils. Because the S809 model in the Delft tunnel was not driven into deep-stall, the S809 data point has been derived from OSU tests corrected by -0.5 deg to match the Delft lift curve. Negative values in *x/c* denote lower-surface ordinates. There seems to be a linear relation between the thickness of the nose and the deep-stall angle. Since the relation should also apply to symmetrical airfoils, the curve essentially goes through the origin:

$$\alpha_{\text{deep-stall}} = 1114 * (y/c) x/c = 0.0125 \quad (2)$$

Conclusions

The results of wind tunnel tests on 5 Delft University airfoils for wind turbines with thickness ranging from 18%*c* to 30%*c* have been presented. The primary design driver for all airfoils was low sensitivity to roughness. The effects on airfoil performance of Gurney flaps of 1%*c* and 2%*c*, of trailing edge wedges with various upstream lengths, of trip wires of 1.2 mm and 2 mm thickness at various leading edge locations and of vortex generators was evaluated. The code XFOIL was modified to improve lift predictions around stall and to calculate the effect of rotation on airfoil performance. The modified version is called RFOIL. It was used to design thick inboard airfoils with 30% and 40% relative thick-

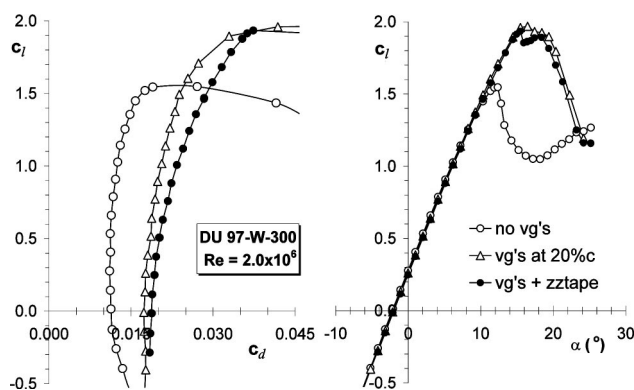


Fig. 21 Effect of vortex generators on the performance of DU 97-W-300 with and without zigzag tape

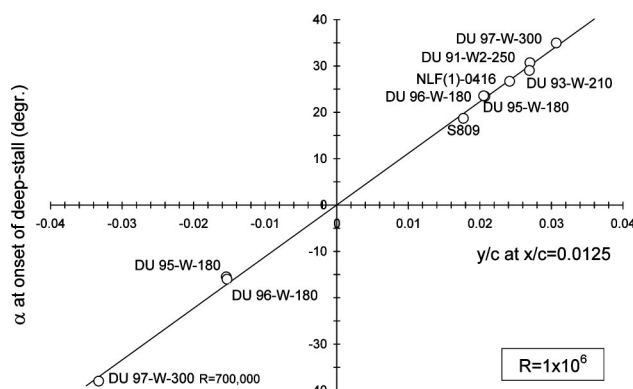


Fig. 23 Correlation of deep-stall angle with leading edge thickness for a number of wind turbine airfoils

ness. The data base of wind tunnel results enabled the correlation of the angle for leading edge separation with the leading edge thickness in terms of y/c at $x/c=0.0125$. This relation appears to be a straight line.

Acknowledgments

The work on DU-airfoils was mainly funded by the European Commission in the framework of the JOULE program and the Netherlands Agency for Energy and the Environment (NOVEM). The assistance of the staff of the Low Speed Laboratory of Delft University is gratefully acknowledged.

References

- [1] Tangler, J. L., and Somers, D. M., 1987, "Status of the Special-Purpose Airfoil Families," *Proceedings Conference Windpower '87, San Francisco, CA, USA*.
- [2] Björck, A., 1990, "Coordinates and Calculations for the FFA-W1-xxx, FFA-W2-xxx, and FFA-W3-xxx Series of Airfoils for Horizontal Axis Wind Turbines," *Report FFA TN 1990-15, Stockholm, Sweden*.
- [3] Timmer, W. A., and van Rooij, R., 1996, "DU 94-W-280, a Thick Airfoil With a Divergent Trailing Edge," *Proceedings European Union Wind Energy Conference, Göteborg, Sweden*.
- [4] Timmer, W. A., and van Rooij, R., 1997, "The Performance of New Wind Turbine Blade Tip and Root Airfoils up to High Angles-of-Attack," *EWEC Dublin, Ireland*.
- [5] Timmer, W. A., and van Rooij, R., 1999, "Measured Section Performance of Rotating Blades as Input to the Design of Inboard Airfoils," *EWEC Nice, France*.
- [6] Timmer, W. A., and van Rooij, R., 2001, "Some Aspects of High Angle-of-Attack Flow on Airfoils for Wind Turbine Application," *EWEC Copenhagen, Denmark*.
- [7] van Rooij, R., "Modification of the Boundary Layer Calculation in RFOIL for Improved Airfoil Stall Prediction," *Report IW-96087R, TU-Delft, the Netherlands*.
- [8] Bosschers, J., Montgomery, B., Brand, A., and van Rooij, R., 1996, "Influence of Blade Rotation on the Sectional Aerodynamics of Rotational Blades," *22nd European Rotorcraft Forum, England*.
- [9] Allen, H. J., and Vincenti, W. G., 1947, "Wall Interference in a Two-Dimensional Wind Tunnel, With Consideration of the Effect of Compressibility," *NACA Report No. 782*.
- [10] Braslow, A. L., and Knox, E. C., 1958, "Simplified Method for the Determination of Critical Height of Distributed Roughness Particles for Boundary-Layer Transition at Mach Numbers From 0 to 5," *NACA Technical Note 436*.
- [11] van Rooij, R., and Timmer, W. A., 2003, "Roughness Sensitivity Considerations for Thick Rotor Blade Airfoils," *41st Aerospace Sciences Meeting, January, Reno, USA Paper no. AIAA-2003-0350*.
- [12] Giguère, P., Lemay, J., and Dumas, G., 1995, "Gurney Flap Effects and Scaling for Low-Speed Airfoils," *AIAA Paper 95-1881, 13th AIAA Applied Aerodynamics Conference San Diego, June*.
- [13] Wentz, Jr., W. H., 1975, "Effectiveness of Spoilers on the GA(W)-1 Airfoil With a High-Performance Fowler Flap," *NASA CR-2538, May*.
- [14] Gault, D. E., 1957, "A Correlation of Low-Speed Airfoil-Section Stalling Characteristics With Reynolds Number and Airfoil Geometry," *NACA Technical Note 3963, Washington, March*.